E-CLOUD EFFECTS ON SINGLE-BUNCH DYNAMICS IN THE PROPOSED PS2 *

M. Venturini†, M. Furman, and J.-L. Vay, LBNL, CA 94720, USA

Abstract

One of the options considered for future upgrades of the LHC injector complex entails the replacement of the PS with the PS2, a longer circumference and higher energy synchrotron. Electron cloud effects represent an important potential limitation to the achievement of the upgrade goals. We report the results of numerical studies aiming at estimating the e-cloud density thresholds for the occurrence of single bunch instabilities.

INTRODUCTION

The requirement for PS2 is to accelerate bunch trains up to 50 GeV kinetic energy (twice the energy reach of PS) in either the 25 ns or the 50 ns bunch spacing configuration, with 4×10^{11} and 5.9×10^{11} particles per bunch respectively.

In addition to space-charge effects [1] and classical instabilities [2], a potential limiting factor to the machine performance is the accumulation of electron cloud. E-cloud can affect the beam dynamics by triggering single or multi-bunch instabilities, or cause a growth of the beam emittance through incoherent effects. Extensive studies of electron cloud formation in the PS2 for various lattice elements, bunch-train structures were reported elsewhere [3]. Here we focus on the investigation of the impact of the electron cloud on the single-bunch dynamics. The study was carried out by macroparticle simulations using the Warp/POSINST code [4]. Preliminarily results were reported in [5].

PHYSICS MODEL

The physics model implemented in Warp is similar to that implemented in other already established codes for the analysis of e-cloud effects on the beam, like HEADTAIL [6]. Warp and HEADTAIL have been extensively benchmarked in the past and further spot-checks were carried out during these studies confirming a generally good agreement with each other. In the model, beam/e-cloud interactions occur at a finite number of discrete interaction points (or 'stations') along the machine circumference, where electrons are effectively confined to a transverse plane orthogonal to the beam orbit. An initially cold and transversely uniform electron distribution is assumed to exist before, and refreshed after, each bunch passage. In an actual machine the form of the distribution and peak value of the e-cloud density is generally strongly dependent on the lattice element type, and often on the exact location along the machine. However, for these studies it is assumed that the electron cloud, concentrated on uniformly distributed stations along the ring circumference, has the same density (peak value and form of transverse distribution) at all stations. The more realistic scenario in which the electron density can vary along the machine, reflecting, in particular, differences of e-cloud accumulation in dipoles and field-free regions as determined by e-cloud build-up codes like POSINST [7] or ECLOUD [8], should be investigated in future work for improved accuracy.

Table 1: Selected lattice/beam parameters used in the Warp simulations

	Extraction	Injection
Kinetic energy (GeV)	50	4
Trans. tunes $Q_{x,y}$	11.8, 6.71	11.8, 6.71
Rms emittance $\gamma\varepsilon_\perp$ (μm)	3	3
Trans. rms sizes $\sigma_{x,y}$ (mm)	1.33, 1.43	4.27, 4.59
Synch. tune Q_s (10^{-3})	1.24	12.1
Long. rms size σ_z (m)	0.30	1.41
Slippage η (10^{-3})	-1.82	-37.5

The electron dynamics during the bunch passage is determined by the self-fields and the fields generated by the beam particles, with an option to pin the electron motion to vertical lines to mimic the dynamics in a dipole magnet. The dynamics of the beam particles is determined by their response to the electron fields at the stations in the 'quasistatic' approximation [4] and optionally to the beam's own fields. The beam particles motion from station to station is modelled by linear transfer maps in the smooth approximation with chromatic effects accounted for by introduction of a phase-advance dependance on the particle momentum. The Poisson equation, yielding the fields generated by the electrons and the protons in the beam slices as the beam steps through each station, is solved on a rectangular grid with metallic boundary conditions. The horizontal and vertical dimensions $2a$=12.5 and $2b$=6.5 cm of the grid were chosen to match the values of the two axes of the proposed elliptical vacuum chamber design.

The goal of the study is to identify threshold values of the e-cloud density for the appearance of single-bunch instabilities. These can generally be captured by relatively short time-scale simulations. The results shown in the following were obtained by simulating the beam dynamics through 10^3 turns (corresponding to about 4.5 ms storage time) at injection and extraction on the assumption of steady (no energy ramping) machine conditions. We did not attempt to assess secular slow-rate emittance growth below instability

* Work supported by DOE under Contract No. DE-AC02-05CH11231 and the US LHC Accelerator Research Program (LARP).

† mventurini@lbl.gov

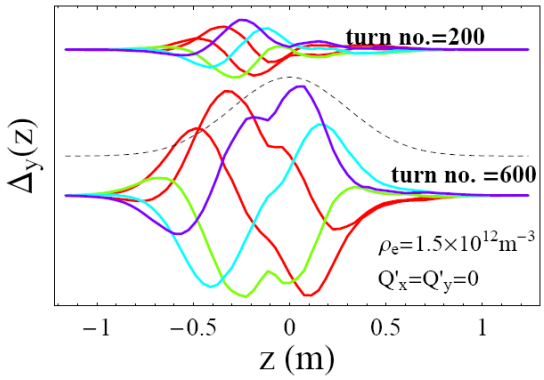

Figure 1: The beam vertical dipole moment along a bunch showing the signature of the head-tail like instability induced by e-cloud. The signal is monitored at one location along the ring for 5 successive bunch passages starting from turn no. 200 (upper set of curves) and 600 (lower set of curves). The dashed line represents the initial bunch longitudinal profile (beam head at $z > 0$).

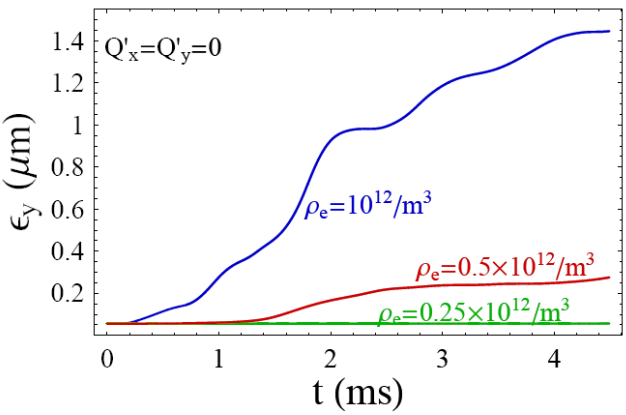

Figure 2: Evolution of the unnormalized vertical emittances for various choices of the e-cloud density ρ_e and vanishing chromaticities at $E = 50$ GeV beam energy.

threshold, which would require implementing a model for energy ramping and a considerably larger computational effort.

Selected machine parameters at injection and extraction used in the present simulations are summarized in Table 1. The beam transverse sizes reported in the table correspond to the nominal rms sizes averaged over the ring circumference for the given design emittances and betatron functions. The negative slippage factors correspond to a purely imaginary value $\gamma_t = 26i$ of the transition gamma factor.

The initial proton beam distribution is assumed gaussian in the 6D phase space (truncated at $\pm 4\sigma$ in the longitudinal direction), matched to the lattice in the absence of e-cloud and space-charge effects. We primarily assumed a nominal bunch population $N_p = 5.9 \times 10^{11}$ protons/bunch but considered a smaller population $N_p = 4.2 \times 10^{11}$ as well for comparison.

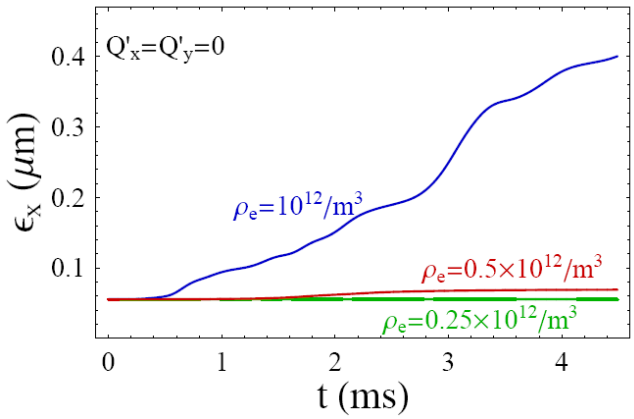

Figure 3: Evolution of the unnormalized horizontal emittances for various choices of the e-cloud density ρ_e and vanishing chromaticities at $E = 50$ GeV beam energy.

SIMULATION RESULTS

Monitoring of the emergence of the instability is primarily done by inspecting the evolution of the bunch centroid in the horizontal and vertical planes. Above threshold the bunch dynamics displays the classic signature of the head-tail instability [9, 10]. This is illustrated by Fig. 1, where we show five turn-by-turn snapshots of the beam slices vertical centroid weighted by the beam longitudinal density after 200 and 600 turns, showing the expected increase in oscillation amplitude in the presence of an instability. Growth in the amplitude of the centroid motion is invariably accompanied by a growth in the beam transverse emittance. Fig.'s 2 and 3 show examples of the evolution of vertical and horizontal emittances at extraction for vanishing chromaticities and various choices of the e-cloud density. The results of a systematic search for the instability threshold are shown in Fig. 4. For vanishing chromaticities the simulations place the instability threshold in the neighborhood of e-cloud density $\rho_e \simeq 0.4 \times 10^{12}$ m^{-3} in the vertical plane (pictures to the right) and slightly above that value in the horizontal plane ($\rho_e \simeq 0.5 \times 10^{12}$ m^{-3}, pictures to the left). We ascribe the discrepancy in the onset of the instability between the two planes to the different values of the transverse tunes, although we would have expected that the significantly larger tune in the horizontal plane would have resulted in a relatively more stable beam motion. The two top-pictures in Fig. 4 report the maximum relative emittance growth measured over 10^3 turns, while the pictures at the bottom report the maximum detected amplitude of centroid oscillation in units of the amplitude of the initial centroid offsets over the same number of turns. (Here and in the other simulations discussed in this paper we generally started the calculation with small beam centroid offsets equal to 10% of the beam rms transverse size). Negative chromaticities of a few units are shown to stabilize the motion as expected for a head-tail like instability in a lattice with negative slippage [11]. Specifically, for the

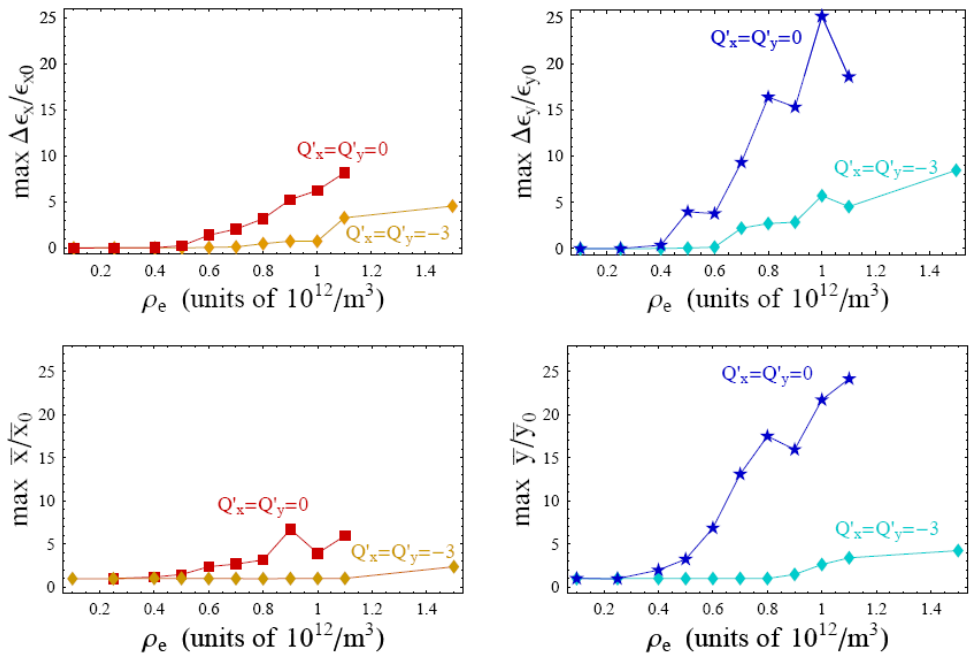

Figure 4: The instability threshold is detected by monitoring the max. variation of emittances (top pictures) and amplitude of the bunch centroid oscillations (bottom pictures) over 1000 turns for increasing values of e-cloud density. Finite negative chromaticities are shown to stabilize the motion. Left and right pictures are for horizontal and vertical motion respectively. $E = 50$ GeV beam energy.

case reported in Fig. 4 chromaticities $Q'_x = Q'_y = -3$ are shown to increase the threshold for emittance growth by 50% while the threshold measured in terms of centroid motion moves upwards by about 100%. We verified that inverting the sign of the chromaticity does not cure and, in fact, may aggravate the instability ($Q'_\alpha = \xi_\alpha Q_\alpha$, with $\alpha = x, y$, where ξ_α is the *relative* chromaticity). The simulations of Fig. 4 were carried out with the motion of the electrons unconstrained in the transverse plane, as is the case in free-field regions. In contrast, in dipoles the electrons gyrate along the vertical field lines effectively suppressing the onset of the instability in the horizontal plane. To approximate this behavior we carried out simulations using the Warp option that enables the pinning of the electron orbits to vertical lines. Results of these simulations are shown in the left picture of Fig. 5, showing the maximum amplitude of the vertical centroid motion oscillations over 10^3 turns (vanishing chromaticities). While there is no sign of instability (or significant emittance growth) in the horizontal plane (data not shown) we can observe a noticeable stabilization of the beam motion in the vertical plane as well, with the instability threshold now moved to about $\rho_e \simeq 0.8 \times 10^{12}$ m^{-3}. Because about half of the PS2 circumference is occupied by dipoles estimates based only on the calculations presented in Fig. 4 (field-free regions) are somewhat pessimistic. Instead, extrapolating these results to a model of machine that combines field free and dipole-occupied regions in the ratio 1:1 we can roughly estimate that, on the assumption that the electron density be the same in bends and field-free regions, we should expect the instability to occur for densities $\rho_e \simeq 2 \times 0.5 \times 10^{12}$ m^{-3} in horizontal plane and $\rho_e \simeq 1.5 \times 0.4 \times 10^{12}$ m^{-3} in the vertical plane.

Varying the bunch population from $N_p = 5.9$ to 4.2×10^{11} did not result in a significant variation in the the instability threshold in the vertical plane while resulting in a somewhat higher threshold in the vertical plane (Fig. 5, center picture).

Finally, we found that at injection the instability is generally milder than at extraction, with the threshold instability in the vertical plane appearing to be about 50% higher, see Fig. 5, right picture. In the same picture also observe a more noticeable difference of behavior in the two planes than observed at extraction, with the horizontal motion appearing relatively more stable. This is not unexpected [12] as the generally unfavorable scaling of instabilities that one would anticipate at lower energy is offset by larger transverse beam sizes that soften the interaction of the beam with the e-cloud. We should caution, however, that the linear approximation assumed for the longitudinal dynamics and a gaussian form assumed for the longitudinal distribution are not necessarily good approximations for the longitudinal dynamics of PS2 at injection, where the bunches fully occupy the rf buckets.

The simulations were carried out using a fairly large number of macroparticles (500k) to represent the proton beam in order to stabilize the simulations outcome from run to run. We used up to 65k macroelectrons to repre-

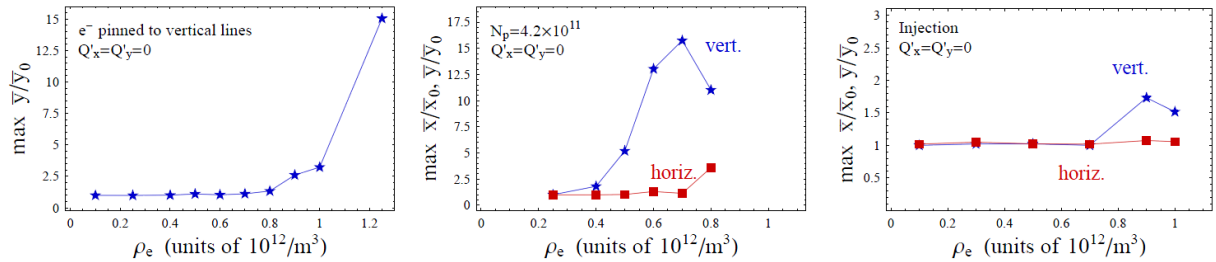

Figure 5: Left picture: max. amplitude of the beam centroid oscillations in the vertical plane *vs.* electron cloud density, with pinning of the electron orbits to vertical lines. Middle picture: decreasing the bunch population from $N_p = 5.9$ to 4.2×10^{11} proton/bunches does not affect the vertical motion significantly while increasing the threshold in the horizontal plane. Right picture: at injection the motion is more stable in both transverse planes. (Left and middle pictures are for the beam at extraction.)

sent the electron cloud starting with realizations of the initial e-cloud density obtained by depositing the macroelectrons on a regular grid. We used 40 stations/turn corresponding to 4 station/betatron wavelength in the vertical plane. Doubling the number of stations did not seem to result in substantially different results. We subdivided the $[-4\sigma_z, 4\sigma_z]$ longitudinal beam support into 64 slices, and generally used a 128×128 grid in the transverse plane. In selected cases we verified that increasing the transverse grid size to 256×256 resulted in somewhat different estimates of emittance growth and amplitude of centroid oscillation above instability threshold but not in a significant difference in the estimate of the critical density at which the instability occurs.

CONCLUSION

The critical values of e-cloud density for the onset of single-bunch instabilities found in this study are within, or close to, the range of densities expected from the e-cloud build-up studies [3].

In particular, the lowest threshold value ($\rho_e = 0.6 \times 10^{12}$ m^{-3}, in the vertical direction) is at the low-end of the interval of estimated e-cloud densities for the case with the more aggressive bunch train structure (25 ns bunch separation). Our results indicate that measures to mitigate the e-cloud accumulation (*e.g.* by decreasing the effective maximum secondary-electron yield below the $\delta_{\max} = 1.3$ reference value used in [3]) would have to be considered for a successful operation of the PS2 ring.

REFERENCES

[1] J. Qiang *et al.*, "Studies of Space Charge Effects in the Proposed CERN" PS2, IPAC 2010, Proceedings.

[2] K. Bane *et al.*, "Impedance Considerations for the Design of the Vacuum System of the CERN PS2 Proton Synchrotron", IPAC 2010, Proceedings.

[3] M. Furman *et al.*, "Electron-cloud Build-up Simulations in the Proposed PS2: Status Report", IPAC 2010, Proceedings.

[4] J-L Vay *et al.*, "Update on E-Cloud Simulations using the Package Warp/Posinst", PAC09 Proceedings (2009).

[5] M. Venturini *et al.*, "E-cloud Driven Single-bunch Instabilities in PS2", IPAC 2010, Proceedings.

[6] G. Rumolo and F. Zimmermann, PRST-AB **5** 121002 (2002).

[7] M. A. Furman and G. R. Lambertson, KEK Proc. 97-17; M. A. Furman and M. T. F. Pivi, PRSTAB **5**, e124404 (2003).

[8] G. Rumolo and F. Zimmermann, "Practical User Guide for ECLOUD," CERN-SL-Note-2002-016 (AP), May 13, 2002.

[9] K. Ohmi, F. Zimmermann, and E. Perevedentsev, Phys. Rev. E, **65** 016502 (2001).

[10] F. Zimmermann, PRST-AB, **7** 124801 (2004).

[11] A. Chao, Physics of Collective Instabilities in High Energy Accelerators, John Wiley & Sons, Inc., New York, 1993.

[12] G. Rumolo *et al.*, Phys. Rev. Lett. **100** 144801 (2008).